

# Synthesis of interstellar $\text{CH}^+$ without OH

S. R. Federman,<sup>1</sup> J. M. C. Rawlings,<sup>2</sup> S. D. Taylor<sup>2</sup> and D. A. Williams<sup>2</sup>

<sup>1</sup>*Department of Physics and Astronomy, University of Toledo, Toledo, OH 43606, USA*

<sup>2</sup>*Department of Physics and Astronomy, University College London, Gower Street, London WC1E 6BT*

Accepted 1996 February 6. Received 1995 December 28; in original form 1995 August 29

## ABSTRACT

Both  $\text{CH}^+$  and OH can be produced in warm gas via endothermic reactions, yet recent observations by Federman, Weber & Lambert indicate little correspondence between the abundances for these molecules. A non-thermal origin for  $\text{CH}^+$  production is therefore suggested. Chemical models of diffuse cloud envelopes that include the presence of Alfvén waves are shown to be consistent with the new observations. In these models,  $\text{CH}^+$  is formed as a result of the streaming of  $\text{C}^+$  ions, which are influenced by the passage of Alfvén waves, relative to the cold background gas. Since the background gas is cold, OH production arises solely from ion–molecule reactions initiated by cosmic ray ionization.

**Key words:** MHD – molecular processes – ISM: abundances – cosmic rays – ISM: kinematics and dynamics – ISM: molecules.

## 1 INTRODUCTION

The  $\text{CH}^+$  radical was one of the first molecules detected in interstellar space, but its production route remains elusive. Much observational work in recent years placed important constraints on the theoretical models used to describe the synthesis of this molecule. Federman (1982a) showed that reactions, occurring in the cold gas where neutral molecules readily form, rapidly decrease the  $\text{CH}^+$  abundance below observed levels. Frisch & Jura (1980) and Lambert & Danks (1986) found that there was a strong correlation between the column density of  $\text{CH}^+$ ,  $N(\text{CH}^+)$ , and the amount of  $\text{H}_2$  in highly excited rotational levels. This correspondence appeared to suggest an association between  $\text{CH}^+$  and hot gas because the excited rotational levels could be populated in observable amounts through collisions at high temperature. Furthermore, Cardelli et al. (1990) noticed that  $N(\text{CH}^+)$  varied inversely with  $N(\text{CN})$ . Since CN production requires large abundances for the precursor molecules, especially CH and  $\text{C}_2$ , its synthesis arises in relatively dense gas (see Federman, Danks & Lambert 1984; Federman et al. 1994), thereby indicating that  $\text{CH}^+$  production primarily occurs in low-density material.

A promising theoretical model involved  $\text{CH}^+$  synthesis behind a shock (Elitzur & Watson 1978, 1980) through the endothermic reaction  $\text{C}^+ + \text{H}_2 \rightarrow \text{CH}^+ + \text{H} - \Delta E$ . One of several problems with this model, however, is that substantial amounts of OH were produced via an analogous reaction. Magnetohydrodynamic (MHD) shocks were invoked

by several groups (Draine & Katz 1986; Pineau des Forêts et al. 1986) because these shocks lessened, but did not remove, the problem with the overproduction of OH. Observations were not able to confirm many of the predictions of these shock models. For instance, Lambert, Sheffer & Crane (1990) were not able to reproduce the velocity structure in terms of components, nor the column density of  $\text{CH}^+$  produced in the shock predicted by the models of Draine & Katz (1986) and Monteiro et al. (1988). Moreover, Gredel, van Dishoeck & Black (1993), and Crawford (1995), did not find the expected velocity shifts between the lines of  $\text{CH}^+$  and CH.

Other observational results suggested the presence of velocity shifts (e.g., Federman 1982a; Allen 1994), but in retrospect the interpretations were affected by data with inadequate signal-to-noise ratios. Two examples illustrate the situation. Federman found a broad, single  $\text{CH}^+$  component toward  $\zeta$  Per that had a velocity intermediate between two CH components. More recent data acquired at very high spectral resolution and good signal-to-noise ratio (Crane, Lambert & Sheffer 1995) reveal that there are two  $\text{CH}^+$  components which correspond to the CH ones. In a similar vein, Allen found a very large difference between the velocities for  $\text{CH}^+$  and CH absorption toward HD53367. The data of Gredel et al. (1993) show weak absorption from the other species at the velocity measured by Allen (1994). Considering the precision of the measurements of Federman (1982a) and Allen (1994), one is led to the conclusion that there is no strong evidence for shifts in excess of

$\sim 1.0\text{--}1.5 \text{ km s}^{-1}$ , which is essentially at the limit of observations today. In the rare case that still arises, it is very likely that weak absorption is masked by too low a signal-to-noise ratio, as discussed above for HD53367 and by Cardelli, Federman & Smith (1991) for gas toward Cep OB3. This fact would also explain the correspondences with the  $K_1$  velocity structure noted by Federman (1980, 1982b).

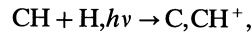
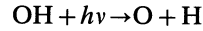
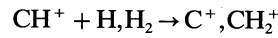
Without the presence of shifts, the shock models are no longer as promising as once believed. The most recent modelling efforts consider gas heated to high enough temperatures to allow the endothermic reaction to proceed, but the high temperature arises through turbulent heating (Duley et al. 1992; Falgarone, Pineau des Forêts & Roueff 1995; Hogerheijde et al. 1995). These models, like the shock models, produce a significant amount of OH as well. New OH observations suggest that  $\text{CH}^+$  production cannot be attributed to heated material. Federman, Weber & Lambert (1996) confirm earlier reports of OH absorption toward  $\sigma$  and  $\zeta$  Per, but they did not detect any OH towards  $\xi$  Per. The limit for OH towards  $\xi$  Per is comparable to the detected amount towards  $\zeta$  Per, but  $\xi$  Per has about 10 times more  $\text{CH}^+$  along its sight line. An enhanced photodissociation rate for OH, of about a factor of 3, is not adequate to explain this factor of 10 difference (Federman et al. 1994). Then, where is the OH associated with  $\text{CH}^+$  production in warm gas toward  $\xi$  Per?

Ultra-high-resolution observations (Lambert et al. 1990; Crawford et al. 1994; Crane et al. 1995; Crawford 1995) clearly reveal non-thermal broadening of absorption features. Moreover, Federman et al. (1994) concluded that the contribution from thermal pressure increases as one probes further into a cloud, but the observations do not reflect this gradient: component velocities are similar for species that probe different portions of a diffuse cloud and linewidths are larger where the thermal pressure is lower. Cloud envelopes, therefore, appear to require another form of pressure, which we consider here to be composed of turbulence created by the superposition of different modes of MHD waves. Since the OH observations described above indicate that hot gas is not involved with the synthesis of  $\text{CH}^+$ , in this paper we explore the possibility that  $\text{C}^+$  ions, which are tied to the magnetic field, attain significant non-thermal motion as a result of the motion of the MHD waves, *but in a region where the surrounding material is cold*. This idea was suggested by Gredel et al. (1993), but they did not perform any detailed calculations to support the premise. Charnley & Butner (1995) suggested that the process may be important in explaining the observed fractionation of deuterated species, but did not discuss the more general effects that MHD waves are likely to have on the chemistry of diffuse clouds.

## 2 MHD CHEMISTRY

We now address the problem of how there can be substantial variations in the observed  $\text{CH}^+:\text{OH}$  ratio along different lines of sight that are believed to have similar physical conditions.

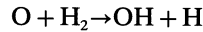
The decoupling of the OH chemistry from that of  $\text{CH}^+$  suggests the presence of non-thermal chemical effects. If we consider the main loss channels for small radicals in diffuse clouds



then it is clear that the conditions required to obtain varying values of the  $\text{CH}^+:\text{OH}$  ratio would have to be somewhat contrived. The differentiation must therefore come about as a result of varying formation efficiencies. In order to obtain the requisite  $\text{CH}^+$  abundance, the endothermic reaction



with  $k = 1.0 \times 10^{-10} e^{-4640/T} \text{ cm}^3 \text{ s}^{-1}$ , must be operating. However, one problem is that the higher temperatures also drive a faster oxygen chemistry, with substantial OH over-production:



( $k = 8.34 \times 10^{-20} T^{2.67} e^{-3160/T} \text{ cm}^3 \text{ s}^{-1}$ ). We therefore have to consider what processes can drive reaction (1) without enhancing the oxygen chemistry. The most likely possibility is that there is some extra, non-thermal, contribution which affects the relative motion of the ions and neutrals. Ion-neutral streaming may occur if MHD waves are present, but only if the ion fluid (which is tied to the MHD waves) is significantly decoupled from the neutral fluid. The relative motion of the fluids leads to drag and has a strongly dissipative effect on the MHD waves. For the purpose of our model we consider the extreme case of the MHD waves being represented by motions in the ion fluid against a static neutral gas background.

## 3 THE MODEL

In order to quantify the effects of non-thermal motions on diffuse cloud chemistry, we developed a highly simplified chemical model of a diffuse cloud boundary layer, defined as a transition zone between the cloud and the intercloud medium where wave dissipation occurs. The model considers the time-dependent evolution of the chemistry at just one point in the cloud envelope. It does not attempt to describe the changing physical and chemical conditions through the regions of intermediate extinction. Rather, we impose a set of conditions that are believed to be representative of the region in which the effects of MHD-enhanced chemistry are significant.

The chemical model uses a limited set of some 83 chemical species chosen so as to be representative of diffuse cloud chemistry. The species are composed of the elements H,

**Table 1.** Elemental abundances used in the models (relative to hydrogen). The entry M refers to the total abundance of low-ionization potential metals, represented by Na in our model.

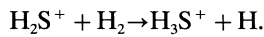
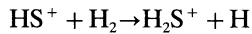
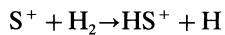
He:	0.076
C:	$2 \times 10^{-4}$
N:	$7.94 \times 10^{-5}$
O:	$3.02 \times 10^{-4}$
M:	$5.2 \times 10^{-6}$
S:	$8 \times 10^{-6}$

He, C, N, O, S and a representative low ionization potential metal, Na. Elemental abundances, based on revised current observational estimates (Savage, Cardelli & Sofia 1992), are given in Table 1. The abundance of Na is set to be the same as that for the equivalent total abundance of metals with low ionization potential.

As we are primarily interested in the chemistry of simple radicals, the species are of limited complexity (up to  $C_3H_3^+$ ,  $H_2CS^+$ ,  $NH_4^+$  etc.) and do not include complex hydrocarbons. Sulphur chemistry is included for comparison with upper limits on  $HS^+$  absorption, and a comprehensive reaction set consisting of some 1071 reactions is drawn from the current UMIST data base (RATE94). It is of interest to note that, of the 3808 reactions contained in the RATE94 data base, only 66 ion–neutral reactions are claimed to have a temperature dependence, and, of those, only 17 have a positive dependence (that is to say, they are faster at higher temperatures). Most of these reactions are included in our model and, in addition to reaction (1), include the charge-exchange reaction

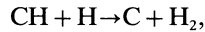


and the hydrogen sulphide chain



In all there are 23 reactions in the set that are affected by ion–neutral streaming.

Certain key chemical rate coefficients have been updated and considerably modified in RATE94 since the earlier releases of the ratefile. In particular, the main loss channel for CH, the exothermic reaction



has a (measured) rate coefficient of  $4.98 \times 10^{-11} \text{ cm}^3 \text{ s}^{-1}$  at 298 K (Harding, Guadagnini & Schatz 1993). We adopt the measured value in our models. Most importantly, the reaction apparently does *not* have an activation energy barrier of 2200 K as had been previously assumed.

To implement the non-thermal enhancements we define an effective temperature for each ion–neutral reaction. Following Draine (1980) and Flower, Pineau des Forêts & Hartquist (1985),

$$kT_{\text{eff}} = kT_{\text{kin}} + \frac{1}{2} \mu v_{\text{in}}^2,$$

where  $k$  is the Boltzmann constant,  $T_{\text{kin}}$  is the thermal kinetic temperature,  $v_{\text{in}}$  is the relative ion–neutral drift speed and  $\mu$  is the reduced mass of the system. In our model we identify  $v_{\text{in}}$  as the rms MHD wave amplitude. Flower et al. (1985) point out that, for linear MHD waves, the thermal motions are three-dimensional whilst the drift is only one-dimensional. A more appropriate expression therefore is

$$\frac{3}{2} kT_{\text{eff}} = \frac{3}{2} kT_{\text{kin}} + \frac{1}{2} \mu v_{\text{in}}^2.$$

This implies that the non-thermal effects are somewhat smaller than in the unmodified form, but it is a more realistic description of the streaming and hence it was adopted in our model.

We set  $A_V$  at 0.3 mag of extinction, which is appropriate to the predominantly atomic diffuse cloud envelope where we postulate that MHD dissipation occurs. In our ‘standard’ model, the  $H_2$  fractional abundance is approximately 10 per cent, consistent with observations of the H-to- $H_2$  transition in diffuse cloud envelopes, so that the endothermic reaction for  $CH^+$  formation proceeds effectively. This is achieved by arbitrarily introducing a shielding factor for the  $H_2$ -dissociating UV flux. The corresponding self-shielding factor reduces the UV flux by  $\sim 7.9 \times 10^{-4}$  and is the same for all of our model runs. CO self-shielding is not included in the model because its abundance is relatively low. The ‘standard’ model has a density of  $100 \text{ cm}^{-3}$ . The kinetic temperature is fixed at 100 K in all of our model runs, a value consistent with theoretical models (Taylor, Hartquist & Williams 1993); however, the precise temperature in the vicinity of 100 K does not have a significant effect on the chemistry.

In the absence of sufficient ion–neutral velocities,  $CH^+$  is formed by direct radiative association:



( $k = 1.7 \times 10^{-17} \text{ cm}^3 \text{ s}^{-1}$ ). With a kinetic temperature of 100 K and an  $H_2$  abundance of 10 per cent, this reaction is faster than reaction (1) when  $T_{\text{eff}} \leq 422 \text{ K}$ , corresponding to an Alfvén speed ( $V_A$ ) of  $\sim 2.2 \text{ km s}^{-1}$ . Observed  $CH^+$  lines tend to have Doppler widths of  $\sim 2.5 \text{ km s}^{-1}$  (Lambert & Danks 1986; Lambert et al. 1990; Crawford et al. 1994; Crawford 1995). Since the non-thermal motion of the  $C^+$  ions can be considered as one-dimensional in our picture, the resulting broadening of the  $CH^+$  line is also one-dimensional. This suggests that the effects of Alfvén speeds as

**Table 2.** Fractional abundances obtained from the models. Two values are shown for each species. The upper and lower values correspond to the equilibrium abundance obtained before and after the addition of MHD ion–neutral streaming respectively. See text for a description of the models.

Species	Model 1	Model 2	Model 3	Model 4	Model 5
$CH^+$	3.3(-12) 5.0(-9)	3.3(-12) 2.8(-9)	3.1(-12) 8.1(-9)	3.3(-12) 1.5(-11)	3.3(-12) 7.2(-8)
CH	1.6(-10) 9.3(-9)	5.7(-11) 1.9(-9)	3.8(-10) 3.6(-8)	1.6(-10) 1.5(-10)	1.6(-10) 1.2(-7)
OH	1.6(-10) 2.7(-10)	9.3(-11) 1.2(-10)	2.6(-10) 5.7(-10)	1.6(-10) 1.6(-10)	1.6(-10) 1.7(-9)
$HCO^+$	3.0(-13) 1.5(-11)	1.6(-13) 4.8(-12)	5.5(-13) 3.8(-11)	3.0(-13) 2.9(-13)	3.0(-13) 2.1(-10)
$O^+$	8.2(-14) 2.6(-12)	8.1(-14) 2.6(-12)	6.9(-14) 2.1(-12)	8.2(-14) 1.1(-13)	8.2(-14) 3.8(-11)
$H^+$	2.8(-9) 1.5(-8)	2.7(-9) 1.5(-8)	2.5(-9) 1.3(-8)	2.8(-9) 9.2(-10)	2.8(-9) 1.8(-7)
$CO^+$	3.1(-14) 7.0(-13)	1.8(-14) 3.9(-13)	4.8(-14) 1.1(-12)	3.1(-14) 3.3(-14)	3.1(-14) 9.6(-12)
$HS^+$	3.6(-14) 1.9(-12)	2.0(-14) 9.8(-13)	6.2(-14) 3.4(-12)	3.6(-14) 2.7(-14)	3.6(-14) 2.9(-10)
HCN	3.3(-14) 2.9(-12)	1.2(-14) 5.8(-13)	8.0(-14) 1.2(-11)	3.3(-14) 3.3(-14)	3.3(-14) 4.2(-11)

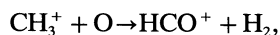
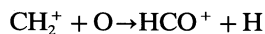
large as  $\sim 4 \text{ km s}^{-1}$  can be explored. We adopt a standard value of  $V_A = 3 \text{ km s}^{-1}$  in our models.

The modelling proceeds in the following way. We initially integrate the chemistry without the non-thermal additions until equilibrium conditions are obtained (after about  $10^5$ – $10^6$  yr). We then introduce the MHD augmentation to the effective temperatures for the relevant reactions and follow the subsequent time-dependent chemical evolution for some  $10^5$  yr, by which time a new equilibrium has been established.

#### 4 RESULTS

The results from the model are presented in Table 2. We do not present the time-dependent evolution of the abundances, as the only features of interest are the time-scales for the abundances to re-adjust to the non-thermal rates. Table 2 gives both the equilibrium fractional abundances relative to hydrogen nuclei before the non-thermal effects are introduced and also the results of the addition of the MHD-enhanced ion–neutral rate coefficients (at equilibrium). The results of the enhancement to the chemistry brought about by the MHD waves can thus be seen by comparing the two entities for each chemical species.

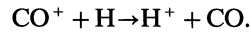
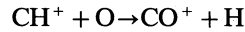
Model 1 is the standard model ( $n = 100 \text{ cm}^{-3}$ ,  $V_A = 3 \text{ km s}^{-1}$ ,  $T_{\text{kin}} = 100 \text{ K}$ ). The effects of changing the density are explored in models 2 ( $n = 50 \text{ cm}^{-3}$ ) and 3 ( $n = 200 \text{ cm}^{-3}$ ), and different Alfvén velocities are used in models 4 ( $V_A = 2 \text{ km s}^{-1}$ ) and 5 ( $V_A = 4 \text{ km s}^{-1}$ ). A fractional ionization of  $2.1 \times 10^{-4}$  results from all of the model runs. The results from the standard model show the huge enhancements in the  $\text{CH}^+$  fractional abundance that are obtained (more than  $1000 \times$ ) whilst the OH fractional abundance is enhanced by a factor of less than  $2 \times$ . Thus, the  $\text{CH}^+:\text{OH}$  ratio changes from 0.02 to 18.5 when MHD enhancements are introduced. Assuming a standard dust-to-gas ratio,  $A_V = 0.3 \text{ mag}$  corresponds to  $N(\text{H}) \sim 6 \times 10^{20} \text{ cm}^{-2}$ , so the ‘before’ and ‘after’  $\text{CH}^+$  fractional abundances correspond to column densities of  $2 \times 10^9$  and  $3 \times 10^{12} \text{ cm}^{-2}$  respectively. These values can be regarded as average values under the assumption that the fractional abundances do not vary much over this small column density. The latter, MHD-derived value is similar to observed ones (e.g., Federman 1982a). The chemistry of CH is affected by changes in the  $\text{CH}^+$  abundance as well. We find that the fractional abundance of CH is enhanced by a factor of  $\sim 58$ , corresponding to  $N(\text{CH}) \approx 5.6 \times 10^{12} \text{ cm}^{-2}$ ; many sight lines have comparable CH column densities (e.g., Federman 1982a).  $\text{HCO}^+$ , which is mainly formed by the reactions



is enhanced by a factor of  $50 \times$ , but the implied column density of  $9 \times 10^9 \text{ cm}^{-2}$  is insufficient to explain its unexpectedly large detected column density on several lines of sight (e.g., Lucas & Liszt 1993; Hogerheijde et al. 1995).

The time-scale for the chemical readjustments is very short (of the order of one year) for those species, such as  $\text{CH}^+$ , which are directly affected by MHD rate enhancements. All other relevant non-chemical time-scales are much longer. Related species re-adjust on longer time-

scales:  $\text{HCO}^+$ ,  $\text{CH}_2$ ,  $\text{CH}_2^+$  (10 yr) and  $\text{CH}_3$  (100 yr). The oxygen chemistry ( $\text{H}_2\text{O}$ ,  $\text{O}^+$ ) is only affected on time-scales of  $10^3$ – $10^4$  yr or even longer ( $\text{H}_3\text{O}^+$ ). These species tend to be affected by the MHD enhancements through a chain of reactions. In Table 2 we can see that there is a substantial increase in the  $\text{O}^+$  fractional abundance. Although partly derived from the temperature dependence of the charge exchange reaction (2), the main cause is the enhancement of the  $\text{H}^+$  abundance brought about by the sequence



The increased  $\text{O}^+$  fractional abundance then drives the oxygen chemistry:



The enhancements are very much smaller, however, than for  $\text{CH}^+$ .

The main effect of varying the density (models 2 and 3) is for the  $\text{H}_2$  abundance to be altered (to 5.6 and 16.7 per cent, respectively, assuming that the shielding factor for  $\text{H}_2$  photodissociation does not change) with corresponding effects on the chemistry. For instance, the CH and  $\text{HCO}^+$  fractional abundances are sensitive to  $\text{CH}_3^+$ , the fractional abundance of which, in turn, is driven by the  $\text{CH}_n^+ + \text{H}_2$  reactions. Model 3 predicts excessive CH fractional abundances. The non-thermal ‘temperature’ is proportional to  $V_A^2$  so, as predicted above, in model 4 ( $V_A = 2 \text{ km s}^{-1}$ ) the non-thermal effects on the chemistry are relatively marginal, whereas model 5 ( $V_A = 4 \text{ km s}^{-1}$ ) predicts excessive  $\text{CH}^+$  and CH fractional abundances, but may be viable at lower densities ( $n = 10$ – $20 \text{ cm}^{-3}$ ). In an additional model, 6, we investigated the sensitivity of our results to the values of the rate coefficients that we used by altering the values of some of the less-well-defined rates. These alterations are summarized in Table 3. The results from model 6 do not show any major differences from the standard model, except for the CH fractional abundance [ $X(\text{CH}) = 5.0 \times 10^{-8}$ ], which is substantially enhanced as a result of the suppression of the  $\text{CH} + \text{H}$  destruction channel. The fractional abundances of  $\text{H}^+$ ,  $\text{O}^+$  and  $\text{CO}^+$  are enhanced by about 50 per cent (relative to model 1), but the abundances of most other species of interest are altered by less than 10 per cent. The results are therefore still consistent with the overall conclusions of this paper that the variations in the  $\text{CH}^+:\text{OH}$  ratio can be caused by non-thermal MHD waves.

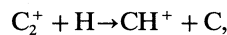
**Table 3.** Values used for rate coefficients (in  $\text{cm}^3 \text{ s}^{-1}$ ) in the models. References: (1) this work; (2) Federman & Huntress (1989); (3) Dubernet et al. (1992); (4) Anicich (1993).

Reaction	Models 1–5	Model 6	Reference
$\text{CH} + \text{H} \rightarrow \text{C} + \text{H}_2$	5(-11)	0	1
$\text{O}^+ + \text{CH} \rightarrow \text{CH}^+ + \text{C}$	3.8(-10)	8.1(-10)	2
$\text{C}^+ + \text{OH} \rightarrow \text{CO}^+ + \text{H}$	7.7(-10)	4.2(-9)	3
$\text{C}^+ + \text{H}_2\text{O} \rightarrow \text{HCO}^+ + \text{H}$	9.0(-10)	2.2(-9)	4
$\text{CO}^+ + \text{H}_2 \rightarrow \text{HCO}^+ + \text{H}$	1.8(-9)	7.3(-10)	4

## 5 DISCUSSION

An alternative way of creating  $\text{CH}^+$  in the absence of OH is the destruction of carbon chain molecules in hot gas. Such molecules have been suggested as candidates for the carriers of the DIBs (Douglas 1977) and their origin possibly lies in the degradation of carbon grains. Taylor & Williams (1993) showed that detectable amounts of  $\text{CH}^+$  along lines of sight without molecular hydrogen could be produced through the shock erosion of grains assuming an alkane such as  $\text{CH}_2$  is the dominant ejected molecule, but this mechanism could not account for the observed column densities of  $10^{12} \text{ cm}^{-2}$  or greater.

If the linewidths of  $\sim 3 \text{ km s}^{-1}$  are caused by a purely thermal gas then temperatures of 5000 K are required. The gas must then have a density of  $\sim 5 \text{ cm}^{-3}$  to maintain pressure balance with the cloud and be composed of atomic hydrogen if OH is not to be produced. We therefore investigated the possibility that under such conditions a carbon chain such as  $\text{C}_4$  can be destroyed to produce  $\text{CH}^+$ . The steady erosion of grains over the lifetime of a cloud ( $\sim 10^6$  yr) cannot produce large column densities of even the injected parent molecule, and certainly not of  $\text{CH}^+$ . Some other mechanisms that produce carbon chains are therefore required in order to account for the observations. They might include the transient injection of grains into the gas, a highly efficient recycling of carbon ions back into grains, or a gas-phase synthesis. Nevertheless we find that, even with the steady erosion of grains, it is possible to enhance the  $\text{CH}^+$  column density by a factor of around 20 over that calculated from synthesis in an atomic gas by reaction (3), through highly endothermic reactions that insert hydrogen atoms into carbon chains. The most important reaction of this type is



where we estimated the reaction rate ( $k = 5 \times 10^{-10} \text{ e}^{-1.5 \times 10^4/T} \text{ cm}^3 \text{ s}^{-1}$ ) and used similar values for other, related, reactions. We find that the  $\text{CH}^+$  abundance is always a factor of 2 bigger than that of CH, and although some  $\text{H}_2$  is produced from  $\text{CH}^+$  the abundance of OH is always 10–20 times less than that of  $\text{CH}^+$ . Although this suggests that some  $\text{CH}^+$  enhancement is caused by carbon chain degradation, the enhancements and the abundance ratios are very much less dramatic than some of the observed variations.

In contrast, our MHD model predicts  $\text{CH}^+$  and CH abundances that are compatible with the observations. The values of the  $\text{CH}^+:\text{CH}$  ratio are particularly close to those observed for many sight lines. Additional CH production through the reaction  $\text{C}^+ + \text{H}_2 \rightarrow \text{CH}_2^+ + h\nu$  at ambient temperatures provides the necessary enhanced column densities for regions rich in molecules. Since our picture does not produce large amounts of OH, cosmic ray induced ion-molecule chemistry in cold gas supplies the observed column densities (see van Dishoeck & Black 1986; Federman et al. 1996). The  $\text{HCO}^+$  and HCN abundances are somewhat lower than those deduced from observations (Lucas & Liszt 1993; Hogerheijde et al. 1995), and the sulphur chemistry yields  $N(\text{HS}^+)$  well below observational limits (Millar & Hobbs 1988; Magnani & Salzer 1991). However, our model is highly simplified and the next step would be to

integrate the effects discussed in this paper into a more physically plausible slab model of a diffuse cloud. It seems likely that some other mechanism is required to account for the  $\text{HCO}^+$  observations. We made some rather arbitrary assumptions about the length-scales over which MHD effects may be important, and we must be careful to consider the energetics of the MHD waves. In the cores of dark clouds, where the fractional ionization is lower ( $\sim 10^{-7}$ ), MHD waves are dissipated on short time-scales (Hartquist et al. 1993) and turbulent support is not seen to exist (Myers & Goodman 1988). In the outermost parts of the cloud, the ionization level is sufficiently high ( $\sim 10^{-1}$ ) for the ionic and neutral fluids to be well coupled. There will be little dissipation in these circumstances, but also little ion-neutral streaming. It is only in the intermediate, dissipative zone that the effects are significant, and this must be incorporated realistically into any slab model of the cloud. However, the mechanism that we propose here is sufficiently efficient to be able to explain the observed  $\text{CH}^+:\text{OH}:\text{CH}$  ratios and their variations from star to star. These findings strongly encourage us to develop the models further.

## ACKNOWLEDGMENTS

SRF acknowledges the hospitality of University College London where most of this work was completed. This work was supported in part by a grant from PPARC.

## REFERENCES

- Allen M. M., 1994, *ApJ*, 424, 754  
 Anicich V. G., 1993, *J. Phys. Chem. Ref. Data*, 22, 1469  
 Cardelli J. A., Sunteff N. B., Edgar R. J., Savage B. D., 1990, *ApJ*, 362, 551  
 Cardelli J. A., Federman S. R., Smith V. V., 1991, *ApJ*, 381, L17  
 Charnley S. B., Butner H., 1995, *Ap&SS*, 224, 443  
 Crane P., Lambert D. L., Sheffer Y., 1995, *ApJS*, 99, 107  
 Crawford I. A., 1995, *MNRAS*, 277, 458  
 Crawford I. A., Barlow M. J., Diego F., Spyromilio J., 1994, *MNRAS*, 266, 903  
 Douglas A. E., 1977, *Nat*, 269, 130  
 Draine B. T., 1980, *ApJ*, 241, 1021  
 Draine B. T., Katz N., 1986, *ApJ*, 306, 655  
 Dubernet M. L., Gargaud M., McCarroll R., 1992, *A&A*, 259, 373  
 Duley W. W., Hartquist T. W., Sternberg A., Wagenblast R., Williams D. A., 1992, *MNRAS*, 255, 463  
 Elitzur M., Watson W. D., 1978, *ApJ*, 222, L141  
 Elitzur M., Watson W. D., 1978, *ApJ*, 236, 172  
 Falgarone E., Pineau des Forêts G., Roueff E., 1995, *A&A*, 300, 870  
 Federman S. R., 1980, *ApJ*, 241, L109  
 Federman S. R., 1982a, *ApJ*, 257, 125  
 Federman S. R., 1982b, *ApJ*, 253, 601  
 Federman S. R., Huntress W. T., 1989, *ApJ*, 338, 140  
 Federman S. R., Danks A. C., Lambert D. L., 1984, *ApJ*, 287, 219  
 Federman S. R., Strom C. J., Lambert D. L., Cardelli J. A., Smith V. V., Joseph C. L., 1994, *ApJ*, 424, 772  
 Federman S. R., Weber J., Lambert D. L., 1996, *ApJ*, in press  
 Flower D. R., Pineau des Forêts G., Hartquist T. W., 1985, *MNRAS*, 216, 775  
 Frisch P. C., Jura M., 1980, *ApJ*, 242, 560  
 Gredel R., van Dishoeck E. F., Black J. H., 1993, *A&A*, 269, 477  
 Harding L. B., Guadagnini R., Schatz G. C., 1993, *J. Phys. Chem.*,

L46 *S. R. Federman et al.*

- 97, 5472  
Hartquist T. W., Rawlings J. M. C., Williams D. A., Dalgarno A., 1993, QJRAS, 34, 213  
Hogerheijde M. R., de Geus E. J., Spaans M., van Langevelde H. J., van Dishoeck E. F., 1995, ApJ, 441, L93  
Lambert D. L., Danks A. C., 1986, ApJ, 303, 401  
Lambert D. L., Sheffer Y., Crane P., 1990, ApJ, 359, L19  
Lucas R., Liszt J., 1993, A&A, 276, L33  
Magnani L., Salzer J. J., 1991, AJ, 101, 1429  
Millar T. J., Hobbs L. M., 1988, MNRAS, 231, 953  
Monteiro T. S., Flower D. R., Pineau des Forêts G., Roueff E., 1988, MNRAS, 234, 863  
Myers P. C., Goodman A. A., 1988, ApJ, 329, 392  
Pineau des Forêts G., Flower D. R., Hartquist T. W., Dalgarno A., 1986, MNRAS, 220, 801  
Savage B. D., Cardelli J. A., Sofia V. J., 1992, ApJ, 401, 706  
Taylor S. D., Williams D. A., 1993, MNRAS, 260, 280  
Taylor S. D., Hartquist T. W., Williams D. A., 1993, MNRAS, 264, 929  
van Dishoeck E. F., Black J. H., 1986, ApJS, 62, 109